



Published in final edited form as:

J Immunol. 2022 February 01; 208(3): 633–641. doi:10.4049/jimmunol.2100139.

Regulation of Cutaneous Immunity In Vivo by Calcitonin Gene-Related Peptide Signaling through Endothelial Cells

Wanhong Ding^{*}, Lori L. Stohl^{*}, Jad Saab[†], Shayan Azizi^{*}, Xi K. Zhou[‡], Devina Mehta^{*}, Richard D. Granstein^{*}

^{*}Department of Dermatology, Weill Cornell Medicine, New York, NY, USA

[†]Department of Pathology and Laboratory Medicine, Weill Cornell Medicine, New York, NY, USA

[‡]Department of Population Health Sciences, Weill Cornell Medicine, New York, NY, USA

Abstract

Calcitonin gene-related peptide (CGRP²) can bias the outcome of Ag presentation to responsive T cells in vitro away from Th1-type immunity and towards the Th2 and Th17 poles through actions on endothelial cells (ECs). To test the in vivo significance of this observation, we engineered a mouse lacking functional CGRP receptors on ECs (EC RAMP1 KO mice). Upon percutaneous immunization to 1-fluoro-2,4-dinitrobenzene (DNFB), stimulated CD4⁺ T cells from draining lymph nodes showed significantly reduced IL-17A expression with significantly increased IFN- γ , IL-4 and IL-22 expression at the protein and mRNA levels compared to control mice. Retinoic acid receptor-related orphan receptor gamma t (ROR γ t) mRNA was significantly reduced while mRNAs for T-box expressed in T cells (T-bet) and GATA binding protein 3 (GATA3) were significantly increased. Additionally, EC RAMP1 KO mice had significantly reduced contact hypersensitivity (CHS) responses and systemic administration of a CGRP receptor antagonist similarly inhibited CHS in wild-type mice. These observations provide compelling evidence that CGRP is a key regulator of cutaneous immunity through effects on ECs and suggest a novel pathway for potential therapeutic manipulation.

Introduction

Calcitonin gene-related peptide (CGRP²) is a 37-amino acid neuropeptide produced by an alternative splicing of the calcitonin gene (1,2) frequently co-expressed with substance P or somatostatin in sensory neurons (3). CGRP is a pleiotropic signaling molecule with many

²Abbreviations used in this article: BIBN, BIBN4096BS; CGRP, calcitonin gene-related peptide; CHS, contact hypersensitivity; CLR, calcitonin receptor-like receptor; CM, complete medium; dDC, dermal dendritic cell; DNFB, 1-fluoro-2,4-dinitrobenzene; EC, endothelial cell; EPC, endothelial progenitor cell; GATA3, GATA binding protein 3; LC, Langerhans cell; DMEC, dermal microvascular endothelial cell; RAMP1, receptor activity modifying protein 1; ROR γ t, retinoic acid receptor-related orphan receptor gamma t; Tx, tamoxifen; T-bet, T-box expressed in T cells (T-bet); VE, vascular endothelial.

Corresponding Author: Richard D. Granstein, M.D., Department of Dermatology, Weill Cornell Medicine, 1305 York Avenue, 9th Floor, New York, NY 10021, Tel: 1-646-962-7546, FAX: 1-646-962-0033, rdgranst@med.cornell.edu.

²Abbreviations used in this article: BIBN, BIBN4096BS; CGRP, calcitonin gene-related peptide; CHS, contact hypersensitivity; CLR, calcitonin receptor-like receptor; CM, complete medium; dDC, dermal dendritic cell; DNFB, 1-fluoro-2,4-dinitrobenzene; EC, endothelial cell; EPC, endothelial progenitor cell; GATA3, GATA binding protein 3; LC, Langerhans cell; DMEC, dermal microvascular endothelial cell; RAMP1, receptor activity modifying protein 1; ROR γ t, retinoic acid receptor-related orphan receptor gamma t; Tx, tamoxifen; T-bet, T-box expressed in T cells (T-bet); VE, vascular endothelial.

functional roles including important immunoregulatory functions (4,5,6). CGRP-containing nerves are distributed throughout various tissues and organs (7), and CGRP is expressed in both the central and peripheral nervous systems (7,8). Many other cell types, including monocytes/macrophages (9), Langerhans cells (LCs, dendritic Ag-presenting cells that reside within the epidermis) (10) and keratinocytes (11), amongst others, can produce CGRP. There are two isoforms of CGRP, α CGRP and β CGRP, that differ by 1 amino acid in the rat and 3 amino acids in humans (2).

With regard to immune and inflammatory processes, CGRP has been shown to regulate Ag-presenting cell function and inhibit the acquisition of immunity to Th1-dominant haptens while augmenting immunity to Th2-dominant haptens (12,13,14). While CGRP has proinflammatory activities, many studies have demonstrated that administration of exogenous CGRP can inhibit the elicitation of inflammation by inflammatory stimuli in vivo (15–18) and, perhaps related to this phenomenon, CGRP inhibits the release of certain chemokines by stimulated ECs (19). Additionally, recent studies have implicated CGRP in the induction of psoriatic inflammation by the TLR7 agonist imiquimod in mice (20,21). In this regard, innervation regulates the expression of certain inflammatory disorders in humans, most notably psoriasis (22,23) which improves or resolves when occurring in an area of skin that becomes denervated. This suggests the possibility that the pathway described herein may represent a mechanism by which the nervous system regulates inflammatory skin disorders. The pathophysiology of psoriatic arthritis also involves innervation (24,25).

Recently, we reported that CGRP can bias the outcome of Ag presentation by epidermal Langerhans cells or blood-derived dendritic cells to responsive T cells in vitro away from Th1-type immunity and towards the Th2 and Th17 poles through actions on endothelial cells (ECs) acting as bystanders (4). In these experiments, the presence of CGRP-treated ECs led to stimulated responding CD4⁺ T cells exhibiting significantly increased expression of IL-17A accompanied by inhibition of IFN- γ , IL-4, and IL-22 expression at both the protein and mRNA levels compared to Ag presenting cultures containing ECs not exposed to CGRP (4). Accordingly, RNA levels of ROR γ t were increased in these T cells along with decreases in mRNA levels for T-bet and GATA3 (4). We also found that CD4⁺ cells expressing cytoplasmic IL-17A were increased in this cell population, whereas cells expressing cytoplasmic IFN- γ or IL-4 were decreased (4). These results involved, at least in part, induction of IL-6 release by ECs induced by CGRP (4). Based on these in vitro observations, we have utilized our inducible, conditional EC-specific RAMP1 knockout mouse model to examine the in vivo relevance of these findings. Functional CGRP receptors result from the association of the *calcitonin receptor-like receptor* (CLR) and *receptor activity modifying protein 1* (RAMP1) (26). Thus, removing RAMP1 disables the CGRP receptor. These mice were generated by crossing mice with floxed RAMP1 with other mice carrying vascular endothelial (VE)-cadherin-Cre ER^{T2}. Administration of tamoxifen early in life to these mice results in loss of RAMP1 from ECs (EC RAMP1 KO mice). In these experiments, Cre⁻, floxed RAMP1 mice (Cre⁻ mice) were used as negative control animals.

Materials and Methods

Animals

Vascular endothelial (VE)-cadherin-CreER^{T2} mice were the generous gift of Shahin Raffi, MD (Weill Cornell Medicine). Sperm containing floxed RAMP1 [full Knockout-First mutant allele (Tm1a) on C57BL/6 background; B6NTac;B6N-Ramp1<tm1a(EUCOMM)Wtsi>/H] was obtained from The Mary Lyon Centre, Harwell Science and Innovation Centre, Oxfordshire, UK. In vitro fertilization of C57BL/6 mice yielded mice heterozygous for the RAMP1 mutant. These mice were crossed with mice expressing Flp to generate mice with the wild-type RAMP1 allele (Tm1c) with loxP flanking exon 2. These mice, bearing the Tm1c allele, were then crossed with VE-cadherin-CreER^{T2} RAMP1^{fl/fl} mice to generate Tm1c/+; Cre/+; flp/+ mice (approximately 1/8 pups). Tm1c/+, Cre/+, Flp/+ were then crossed with Tm1c/Tm1c mice to generate the Tm1c/Tm1c, Cre/+ line. Treatment with tamoxifen (see below) yields the EC RAMP1 KO mice. Mice carrying the floxed RAMP1 but not the (VE)-cadherin-CreER^{T2} allele were used as controls (Cre⁻). Mice with the wild-type RAMP1 were also bred with VE-cadherin-CreER^{T2} mice to yield wild-type Cre⁺ wild-type RAMP1 mice as controls for some experiments. These mice are on a C57BL6/N background and were generated by the Mouse Genetic Core transgenic facility of Memorial Sloan-Kettering Cancer Center (MSKCC). Bred mice were genetically initially assessed by agarose gel-based PCR. Toe or tail specimens were obtained and placed in 75 μ L of lysis buffer (25 mM sodium hydroxide with 0.2 mM EDTA) and incubated at 94°C for 45 minutes. Then, add 75 μ L of neutralization buffer (40 mM Tris HCl) was added, mixed well, and spun down; genomic DNA was then harvested. One-half μ L unpurified DNA from each sample were used for PCR. The PCR program was as follows: Initial denature for 3 min at 94°C, followed by 40 cycles of denaturation for 15s at 94°C, annealing for 90s at 68°C, and completion for 7 min at 72°C. Primers for target gene recombination were Tm1a/Tm1c primers: RAMP1: 5'-GCCTTTTCAAAGCACAGTGG-3' forward, 5'-GTCACATGGCATCCA CAGAC-3' reversed, Mut-R1 5'- GAACTTCGGAATAGGAACTTCG-3; Tm1d primers - 5'CAS-F1 AAGGCGCATAACGATAC CAC, 3'LOXP-R1 ACTGATGGCGAGCTCAGACC (using these 2 primers, Tm1d is 174 base pairs and Tm1c is 1000bp). PCR products were resolved on a 2% agarose gel at 130V for 45 ~ 50 minutes. In later experiments, qRT-PCR was used for genetic analysis (Transnetyx).

The mice were bred by the Colony Management Group at MSKCC. Some experiments were performed with BALB/c mice obtained from The Jackson Lab. All mice for experiments were maintained in the Weill Cornell Medical College animal facility under specific pathogen-free conditions, food and water ad libitum, and under a standard 12 h photoperiod at a constant temperature of 21°C. All experiments were conducted in compliance with all relevant ethical regulations and were approved by the Institutional Animal Care and Use Committee of the Weill Cornell Medical College.

Reagents

Tamoxifen free base (Tx), sunflower seed oil, CGRP receptor antagonist BIBN4096BS, 1-fluoro-2,4-dinitrobenzene (DNFB), collagenase A and DNase 1 were purchased from

Millipore Sigma; anti-mouse CD3 mAb and anti-mouse CD28 mAb were from BD Biosciences.

Media

Complete medium (CM) consisted of RPMI 1640 (Mediatech), 10% FBS (American Type Culture Collection), 100 U/ml penicillin, 100 µg/ml streptomycin, 0.1 mM nonessential amino acids, 0.1 mM essential amino acids, 2 mM L-glutamine, 1 mM sodium pyruvate, and 10 mM HEPES buffer (all from Mediatech).

Induction of recombination

Tx was prepared in a vehicle of sunflower oil at a concentration of 20 mg/ml by shaking at 37°C for 1-2 hours until completely dissolved and then stored in a light-blocked condition at 4°C for the duration of injections. Experimental mice were transferred from MSKCC to the mouse hazard room at Weill Cornell Medicine at 10-12 days-old for use. VE-cadherin-CreERT2 RAMP1^{fl/fl}, Cre⁻ mice and Cre⁺ wild-type RAMP1 mice were injected i.p. with 50 or 100 µL of Tx stock solution or with vehicle once every 24 hours for a total of 3 or 4 consecutive days at age 2 weeks and again at age 3 weeks. Treatment of VE-cadherin-CreERT2 RAMP1^{fl/fl} mice with Tx results in loss of RAMP1 from endothelial cells (EC RAMP1 KO mice). Recombination was monitored either by the agarose gel method or qRT-PCR, as described above.

Preparation of dermal microvascular endothelial cells (DMECs), Langerhans cells (LCs), dermal dendritic cells (dDCs) and CD4⁺ T cells for RAMP1 gene expression

Isolation of DMECs: DMECs were prepared from skin obtained as described below (see preparation of LCs), skins were incubated one hour in Ca²⁺/Mg²⁺-free PBS containing 1 U dispase/ml. epidermal sheets were mechanically removed, the remaining dermis was washed in PBS with Ca²⁺ and Mg²⁺ 5 times and incubated for 2-3 hours in a digestion buffer containing 2 mg/ml collagenase A, 100 µg/ml of DNase 1 and 1% BSA in Ca²⁺/Mg²⁺-PBS. The resulting suspension was filtered through a 100, 70 and 40 µm nylon mesh sequentially (VWR) and washed three times with PBS with Ca²⁺ and Mg²⁺ containing 1% BSA. Cells were incubated for 10 minutes with FcR Blocking Reagent (Cat no. 130-092-575, Miltenyi Biotec) to block Fc receptors. Then, PE-conjugated anti-mouse CD31 (MEC 13.3, BD Biosciences) was added to a concentration of 5 µg/ml and APC-conjugated anti-mouse CD45 mAb (30-F11, BD Biosciences) was added to a concentration of 5 µg/ml followed by incubation for 30 min at 4°C. They were then washed twice, resuspended in 1X cold PBS with Ca²⁺ and Mg²⁺ containing 80 µg/ml of DNase 1 and 1% BSA. DMECs were isolated by sorting for CD31⁺CD45⁻ dermal cells with the BD Influx cell sorter (BD Biosciences).

Isolation of LCs: Epidermal cells were prepared using a modification of a standard protocol¹². Truncal skin of mice were shaved with electric clippers and chemically depilated. Subcutaneous fat and panniculus carnosus was removed by blunt dissection. Skin was floated dermis-side down for one hour in Ca²⁺/Mg²⁺-free PBS containing 0.5 U dispase/ml (BD Biosciences) and 0.38% trypsin (Mediatech). Epidermal sheets were collected by gentle scraping, washed, and dissociated by repetitive pipetting in HBSS (Mediatech) supplemented with 2% FBS. Epidermal cells were filtered through a 40-µm

cell strainer (BD Biosciences) to yield epidermal cells containing 2-3% LCs. Epidermal cells were incubated for 10 minutes with FcR Blocking Reagent (cat. no. 130-092-575, Miltenyi Biotec) to block Fc receptors. Then, PE conjugated anti-mouse I-A^b mAb (clone AF6-120.1, BD Biosciences) was added followed by addition of Alexa Fluor® 488 anti-mouse CD45 mAb (clone S18009D, Biolegend) and APC anti-mouse CD31 mAb (clone MEC 13.3, BD Biosciences), each to 5 µg/ml, followed by incubation for 30 min at 4°C. They were then washed twice and resuspended in cold PBS containing 80 µg/ml of DNase 1. LCs were isolated by sorting for epidermal cells expressing I-A^b and CD45 but not expressing CD31 and sorting with the BD Influx cell sorter (BD Biosciences).

Isolation of dermal dendritic cells: Dermis was obtained from skin as described above (see preparation of DMECs). Dermal fragments were washed in Ca²⁺/Mg²⁺-free PBS for at least 5 times and incubated for 2-3 hours in a digestion buffer containing 2 mg/ml collagenase A, 100 µg/ml of DNase 1 and 1% BSA in Ca²⁺/Mg²⁺-free PBS. The resulting suspension was filtered through a 100, 70 and 40 µm nylon mesh sub-sequentially and washed three times with Ca²⁺/Mg²⁺-free PBS containing 1% BSA. Dermal cells were incubated for 10 minutes with FcR Blocking Reagent (cat. no. 130-092-575, Miltenyi Biotec) to block Fc receptors. Then, PE-conjugated anti-mouse I-A^b (AF6-120.1, BD Biosciences) was added to 5 µg/ml and APC conjugated anti-mouse CD11c mAb (BD Biosciences, 117310) was added to 5 µg/ml; cells were then incubated for 30 min at 4°C. followed by washing twice and resuspension in cold PBS containing 80 µg/ml of DNase 1 and 1% BSA. I-A^bCD11c⁺ dermal dendritic cells were then isolated by FACS sorting with the BD Influx cell sorter (BD Biosciences).

Isolation of CD4⁺ T cells: Spleens of mice were mechanically disrupted and passed through a 70-µm nylon mesh to yield a single-cell suspension. CD4⁺ cells were isolated by depletion of nontarget cells. The nontarget cells were indirectly magnetically labeled with a mixture of biotin-conjugated mAbs (CD8a, Cd11b, CD11c, CD19, CD45R (B220), CD49b (DX5), CD105, anti-MHC class II, Ter-119 and TCR-γ/δ) as primary labeling reagent, and anti-biotin mAb conjugated to microbeads, as secondary labeling reagent (CD4 T Cell Isolation Kit, Mouse, Miltenyi Biotec, no. 130-104-454). The magnetically labeled nontarget cells were held on a MACS column in the magnetic field of a MACS separator, whereas the unlabeled CD4⁺ T cells passed through the column (Miltenyi Biotec)

Sensitization of mice and elicitation of contact hypersensitivity (CHS)

Ten EC RAMP1 KO mice and 10 Cre⁻ mice were shaved on the dorsum with electric clippers, half of both sets of mice were immunized by application of 25 µl of 0.5% DNFB in acetone:olive oil (4:1) to the shaved dorsum and the other half painted with acetone:olive oil (4:1) alone. On day 7, 5 µl of 0.2% DNFB 0.2% in acetone:olive oil (4:1) was applied to each side of each ear of all mice. Ear thickness was measured before ear painting and 24 and 48 h later using an engineer's spring-loaded micrometer (Mitutoyo). Mice were euthanized after the 48-hour ear swelling assessment and ears removed and placed in 10% formalin for histological analysis.

Additional experiments were performed examining the ability of administration of the CGRP inhibitor BIBN4096BS to wild-type mice to influence the expression of contact hypersensitivity. Wild-type mice (BALB/c) were injected intraperitoneally with 100 μ l PBS containing 15 μ g BIBN4096BS or PBS alone one-hour before and one-hour after immunization with DNFB as above or were mock-immunized with diluent alone. One-week later 15 μ g BIBN4096BS in 20 μ l of PBS was injected into the base of each ear followed 30 minutes later by challenge of each ear with application of DNFB and assessment of 24- and 48-hr ear swelling as above. Control mice were similarly treated but injected with diluent alone instead of BIBN4096BS.

Histological analyses

The inflammatory infiltrate in ears of EC RAMP1 KO mice and Cre⁻ mice immunized and challenged as above, harvested after the 48-hr ear swelling measurement, was examined histologically in a blinded fashion with slides stained with hematoxylin and eosin (Slides were prepared at the Laboratory of Comparative Pathology (LCP) of the Center for Comparative Medicine and Pathology at Weill Cornell Medicine). The total inflammatory infiltrate, the neutrophilic infiltrate and the lymphocytic infiltrates was scored in a blinded fashion on a semi-quantitative fashion as follows. For Overall Infiltrate: 1+: Baseline “normal” appearing section, 2+: Single focus of mildly dense inflammation, 3+: Two or more discontinuous/separate foci of mildly dense inflammation, 4+: Two or more discontinuous/separate foci of moderately dense inflammation, 5+: Diffuse inflammation with up to moderate density, 6+: Diffuse inflammation with high density. For Individual Neutrophil or Lymphocyte Scoring Criteria: Not Scored, Cells Not Identified or Within Normal Limits, 1+: Present but rare cells, 2+: Mild density of cells, 3+: Moderate density of cells, 4+: High density of cells. Images for publication were prepared by scanning slides with the Aperio GT450 Automated High Capacity Digital Pathology Slide Scanner (Leica Biosystems).

Preparation of supernatants conditioned by CD4⁺ T cells stimulated with anti-CD3 and anti-CD28

Ten EC RAMP1 KO mice and 10 floxed Cre⁻, RAMP1 mice (Cre⁻ mice) were shaved on the dorsum with electric clippers; half of both sets of mice were immunized by application 10 μ l of 1% DNFB in acetone:olive oil (4:1) to each side of the shaved superior dorsum and the other half were painted with vehicle alone. Three days after DNFB immunization, mice were sacrificed and draining lymph nodes (cervical, brachial and axillary) were removed. Lymph nodes were mechanically disrupted and passed through a 70- μ m nylon mesh to yield a single-cell suspension. CD4⁺ T cells were isolated as described above. Ninety-six-well flat-bottom plates were treated with 10 μ g/ml anti-mouse CD3e mAb (145-2C11, BD Biosciences) in PBS overnight and washed. T cells were cultured (3×10^5 cells/well) in 250 μ l CM containing 2 μ g/ml anti-mouse CD28 mAb (BD Biosciences, 553294). Supernatants were collected 72 h after stimulation, and cytokine contents were determined.

Cytokine determinations

Supernatant IL-17A and IL-4 levels were determined by sandwich ELISA following the manufacturer’s instructions (IL-17A, R&D Systems, DY421; IL-4, R&D Systems, DY404).

IL-22 ELISA kits were purchased from Antigenix America (cat. no. RMF222CK). IFN- γ production in cultured medium was measured by a sandwich ELISA using purified rat anti-mouse IFN- γ capture mAb (XMG1.2, BD Biosciences), biotinylated rat anti-mouse IFN- γ detection mAb (XMG1.2, BD Biosciences,) avidin-horseradish peroxidase (HRP) (BD Biosciences, no. 554066) and 3,3',5,5' tetramethylbenzidine substrate (TMB) (BD OptEIA Reagent Set, Biosciences, no. 555214), read at 405 nm.

Reverse transcriptase-polymerase chain reaction (real-time PCR)

RAMP1 gene expression analysis: Total mRNA was extracted from ECs, dermal dendritic cells, LCs and CD4⁺ T cells using the RNeasy Plus Mini Kit (Qiagen); DNA eliminator columns were used to eliminate any contamination with genomic DNA. cDNA was synthesized using a high-capacity RNA-to-cDNA kit according to the manufacturer's instructions (SuperScript VILO cDNA Synthesis Kit; Invitrogen). The primers for murine RAMP1 were designed to span the junction between exon 1 and exon 2 (Ref seq#: NM_001168392): (5'-GGATGAGAGTCCCATAGTCAGG-3' forward and 5'-GGGGCTCTGCTTGCCAT-3 reverse). Expression was performed using PrimeTime primers (Integrated DNA Technologies) and was normalized to glyceraldehyde 3-phosphate dehydrogenase (5'-GTGGAGTCATACTGGAACATGTAG-3' forward; 5'-AATGGTGAAGGTCCGGTGTG-3' reverse). PCR was performed with Power SYBR Green PCR Master Mix (Applied Biosystems), and an ABI 7900HT instrument (Applied Biosystems).

Intracellular cytokine gene expression analysis for CD4⁺ T cells: EC RAMP1 KO and Cre⁻ control mice were sensitized with DNFB. Three days later CD4⁺ T cells were isolated from draining lymph nodes and were stimulated with anti-CD3 mAb and anti-CD28 mAb. Twelve hrs later, total RNA was isolated, and RT-PCR was performed using methods as described above. All of the PrimeTime primers were purchased from Integrated DNA Technologies. Murine IL-17A (5'-GAGCTTCCCAGATCACAGAG-3' forward; 5'-AGACTACCTCAACCGTTCCA-3' reverse), IFN- γ (5'-GAGCTCATTGAATGCTTGGC-3' forward; 5'-CAGCAACAACATAAGCGTCAT-3' reverse), ROR γ t (5'-TCCCACATCTCCCACATTG-3' forward; 5'- -3' reverse) and GATA3 (5'-GTCCCCATTAGCGTTCCTC-3' forward; 5'-CCTTATCAAGCCCAAGCGAAAATGTCTGCAAGTCCTTCCG-3' reverse), T-bet (5'-CAAGACCACATCCACAAACATC-3' forward; 5'-TTCAACCAGCACCAGACAG-3' reverse), IL-4 (5'-TCTTTAGGCTTCCAGGAAGTC-3' forward; 5'-GAGCTGCAGAGACTCTTTTCG-3' reverse), IL-22 (5'-AATCGCCTTGATCTCTCCAC-3' forward; 5'-GCTCAGCTCCTGTCCACATC-3' reverse). Expression of each cytokine and transcription factor was normalized to glyceraldehyde 3-phosphate dehydrogenase (primer sequence above).

Western blotting.

RAMP1 protein expression was detected by Western blotting with a monoclonal antibody specific to RAMP1. DMECs were isolated from both Cre⁻ and RAMP1 KO mice by FACS sorting, as above. After washing two times with cold PBS, EC were lysed by adding 50 ml of cell lysis buffer containing 20 mM Tris-HCL, pH 7.5; 150 mM NaCl; 1mM Na₂EDTA; 1

mM EGTA; 1% Triton; 2.5 mM sodium pyrophosphate; 1 mM glycerophosphate; 1mM Na₃VO₄; 1mg/ml leupeptin, 1mM phenylmethylsulfonylfluoride (Cell Signaling). Cells were then sonicated for 5 seconds 5 times with cooling on ice between sonication. Cell lysates were then centrifuged for 5 minutes. The protein concentration in each sample was determined by a NanoDrop Spectrophotometer (ND-1000, NanoDrop Technologies). Equal amounts of protein (20 µg) of cell lysate from each sample were mixed with 3x Blue Loading Buffer (Cell Signaling) with 40 mM dithiothreitol and were separated on a Mini-PROTEAN Precast SDS-PAGE gel (Bio-Rad), followed by electrotransfer to a nitrocellulose membrane (Bio-Rad). The membrane was blocked with EveryBlot Blocking Buffer (Bio-Rad) for 15 minutes and then washed for 5 minutes 3 times with 1X TBST buffer (Tris-buffered saline buffer, 0.1% Tween 20; Bio-Rad), followed by probing with 1:1,000 dilution of rabbit anti-mouse recombinant anti-RAMP1 antibody (clone EPR10867, Abcam) or with 1:10,000 dilution of rabbit anti-mouse recombinant anti-GAPDH (clone EPR16891, Abcam) overnight at 4°C with. After washing 3 times with 1X TBST, the membrane was probed with 1:10,000 diluted horseradish peroxidase-conjugated goat anti-rabbit IgG (cat. no. STAR208P, Bio-Rad) at room temperature for 1 h. GAPDH was used as the loading control. The protein signals were detected using an enhanced chemiluminescence ECL mixture (Clarity Western ECL Substrate, Bio-Rad) and recorded by a Bright CL 1000 (Invitrogen) imaging system.

Biostatistics

For analysis of the study endpoints including supernatant cytokine contents, CHS (ear swelling) responses, cellular infiltrates observed on histologic sections, and expression of specific mRNAs, linear mixed-effects regression was used to estimate levels of an endpoint in each treatment group while accounting for potential within experiment and within mouse correlations depending on the design of the experiments. Simultaneous testing of general linear hypotheses testing was used to evaluate the contrasts of interest. P-values were adjusted for multiple comparisons by controlling the false discovery rate. Cytokine and mRNA expression data were log transformed prior to the analysis to ensure the underlying model assumptions were satisfied. All statistical analyses were carried out using R (<https://www.r-project.org/>). All p-values were two-sided.

Results

RAMP1 expression is deficient in cutaneous microvascular ECs but not in LCs, dermal dendritic cells (DDCs) or CD4⁺ T cells from EC RAMP1 KO mice

Initial experiments examined the expression of RAMP1 mRNA in ECs derived from EC RAMP1 KO mice and ECs derived from identically treated RAMP1 floxed but Cre⁻ mice. ECs from EC RAMP1 KO mice had substantially reduced expression of RAMP1 compared to ECs from identically treated Cre⁻ mice (Supplemental Fig. 1A). Epidermal Langerhans cells and dermal dendritic cells isolated from these two categories of mice showed no difference in expression of RAMP1 (Supplemental Fig. 1B and 1C). Surprisingly, RAMP1 expression in CD4⁺ T cells isolated from the spleens of EC KO mice showed a small but significant increase in RAMP1 expression compared to CD4⁺ T cells from Cre⁻ mice (Supplemental Fig. 1D). By Western blot, ECs from EC RAMP1 KO mice also expressed

greatly reduced expression of RAMP1 compared to ECs from identically treated Cre⁻ mice (Supplemental Fig. 1E).

Histologic sections of EC RAMP1 KO mouse skin and Cre⁻ mouse skin were stained with periodic acid-Schiff plus diastase to look for differences in vascular morphology by light microscopy. Examination of these sections by an experienced dermatopathologist was performed but no differences in morphology were noted by this technique.

After percutaneous immunization of EC RAMP1 KO mice to DNFB, non-specifically activated CD4⁺ T cells from regional lymph nodes exhibit significantly reduced production of IL-17A and significantly increased production of IFN- γ , IL-4 and IL-22

The next set of experiments examined cytokine expression in CD4⁺ cells isolated from draining lymph nodes of EC RAMP1 KO mice and Cre⁻ control animals immunized to DNFB. DNFB or diluent alone was applied to the shaved dorsa of groups of each type of mice. Three days later, mice were euthanized and draining lymph nodes harvested. A single-cell suspension of CD4⁺ T cells from the draining lymph nodes was obtained by magnetic antibody techniques. Cells were placed in culture and stimulated with anti-CD3 and anti-CD28 mAbs. Supernatants were harvested after 72-hours and assayed by enzyme-linked immunosorbent assay (ELISA) for cytokine contents. Cells from immunized EC RAMP1 KO mice produced significantly less IL-17A compared to immunized Cre⁻ control mice while production of IFN- γ , IL-4, and IL-22 was significantly increased (Fig. 1). A small but significant reduction in IL-17A production was also seen in non-immunized mice as was a significant increase in IL-22 production. Control experiments were performed in a similar manner after administering Tx to mice expressing the wild-type RAMP1 alleles (no floxing) with and without VE-cadherin-CreER^{T2}. No differences in production of IL-17A, IFN- γ , IL-4 or IL-22 was observed between mice expressing wild-type RAMP1 with or without the presence of VE-cadherin-CreER^{T2} (Supplemental Fig. 2).

After percutaneous immunization of EC RAMP1 KO mice to DNFB, non-specifically activated CD4⁺ T cells from regional lymph nodes exhibit a significantly reduced levels of mRNA for IL-17A and ROR γ t with significantly increased levels of mRNA for IFN- γ , T-bet, IL-4, GATA3 and IL-22

In other experiments, examination of mRNA levels for cytokines and relevant transcription factors in CD4⁺ T cells from draining lymph nodes was performed. Groups of EC RAMP1 KO mice and Cre⁻ control mice were similarly immunized. Three days later, draining lymph nodes were harvested. CD4⁺ T cells were isolated and stimulated for 12 hours with anti-CD3 mAb and anti-CD28 mAb as in Methods. Then, total mRNA was prepared and quantitative RT-PCR was performed for mRNAs of interest. As shown by the data in Fig. 2, draining lymph nodes from EC RAMP1 KO mice showed significantly less expression of mRNAs for IL-17A and the Th17-associated transcription factor ROR γ t compared to Cre⁻ control mice while expression of mRNAs for IFN- γ and the Th1-associated transcription factor T-bet, mRNAs for IL-4 and the Th2-associated transcription factor GATA3, and IL-22 mRNA were significantly increased.

The CHS response is significantly reduced in EC RAMP1 KO mice

We also examined CHS responses in EC RAMP1 KO mice. Groups of EC RAMP1 KO mice and Cre⁻ control mice were each immunized by application of DNFB to the shaved dorsum or were mock-immunized with diluent alone. Seven days later, mice were challenged by application of DNFB to the ears and the CHS response quantified by measurement of 24- and 48-hour ear swelling. As shown by the data in Fig. 3A, EC RAMP1 KO mice had a substantially and significantly lesser CHS response, measured by 24- and 48-hour ear swelling, compared to Cre⁻ control mice. Histologic assessment of the ears revealed a significant reduction in the total inflammatory cell response, a significant reduction in the neutrophil infiltrate and a trend toward a lesser lymphocyte infiltrate in ear skin from immunized EC RAMP1 KO mice compared to Cre⁻ mice (Fig. 3B). In Fig. 3C, photomicrographs of a representative section from the ear of a mouse from each group taken 48-hours after challenge (Immunized Cre⁻, Immunized EC RAMP1 KO, Non-Immunized Cre⁻ and Non-Immunized EC RAMP1 KO) are shown. Note that the ear from the immunized Cre⁻ mouse is thicker than the ear from the immunized EC RAMP1 KO with more edema and a thicker dermis with greater inflammatory cell infiltrate. Also, please note that we have chosen representative areas for each photomicrograph. There is variation in the density of the inflammatory infiltrate in each section. The data set from the blinded evaluation of the infiltrate in sections from each ear taken from each mouse is shown in Supplemental Table 1.

A control experiment was also performed in which VE-cadherin-CreER^{T2} RAMP1^{fl/fl} mice and RAMP1^{fl/fl} without Cre mice (Cre⁻ mice) were injected with vehicle alone instead of Tx at 2 and 3 weeks of age and then immunized and challenged as above. As shown in Supplemental Fig. 3, no difference in ear swelling was seen in immunized VE-cadherin-CreER^{T2} RAMP1^{fl/fl} mice compared to RAMP1^{fl/fl} no Cre mice treated with vehicle alone instead of Tx.

Systemic administration of a CGRP inhibitor significantly reduces CHS responses

To further examine the role of CGRP signaling in CHS, we utilized the small molecule competitive inhibitor of CGRP BIBN4096BS (BIBN, also known as olcegepant). Additional experiments were performed examining the ability of administration of this CGRP inhibitor to wild-type mice to influence the expression of CHS. Mice were injected intraperitoneally with BIBN one hour before and one hour after immunization with DNFB by application to the shaved dorsum and one week later BIBN was injected into the base of each ear followed 30 minutes later by challenge of each ear with application of DNFB. Control mice were similarly treated but injected with diluent alone instead of BIBN. Other groups of control mice were treated identically to the groups described above but were mock-immunized with vehicle alone. As shown in Fig. 4, mice injected with BIBN at immunization and elicitation of immunity had a significantly reduced CHS response compared to control mice injected with PBS alone instead of BIBN.

Discussion

These data demonstrate that CGRP-signaling through ECs has a number of profound immunologic effects. With regards to CD4⁺ T cell responses, CGRP-signaling through ECs appears to play an important role in the spectrum of Th cells that result from immunization. These in vivo data demonstrate that CGRP-signaling through ECs favors the differentiation of IL-17A-expressing Th cells (Th17 cells) while reducing the generation of IL-4 expressing (Th2), γ -interferon (IFN- γ)-expressing (Th1) and IL-22-expressing (Th22) Th cells. These observations are quite similar to in vitro experiments in which ECs exposed to CGRP in vitro and then added to Ag-presenting cultures led to similar changes in the spectrum of T helper cells generated in these cultures compared to addition of ECs not pre-treated with CGRP (4). Thus, we believe that the changes in the generation of subsets of Th cells in the regional lymph nodes reported herein are the in vivo counterpart to these in vitro results. Since generation of Th subsets is likely occurring in the lymph nodes, the CGRP signaling effects we are observing in vivo is likely due to ECs in the lymph nodes. Of course, in our current in vivo experiments this is uncertain. We plan additional experiments utilizing tissue transplants between control and EC RAMP1 KO mice for the near future to attempt to determine if this is the case. The current report demonstrates the in vivo significance of the in vitro observations and suggests that CGRP may play a regulatory role in disorders characterized by inappropriate Th17 cell activity. In this regard, it has been reported that ECs in lesions of psoriasis, a disease involving Th17 cell activity (27), have CGRP on their surfaces (10) and that psoriasis patient have elevated plasma levels of CGRP (28). The possibility that therapeutic manipulation of this pathway may benefit disorders characterized by inappropriate Th17/IL-17A activity should be examined.

The profound changes in CHS response in the EC-RAMP1 KO mice are also of considerable interest. Whether this observation relates to the changes in T helper cell generation discussed above remains unknown. However, since CGRP is a potent vasodilator, it is also possible that CGRP-signaling in the skin vasculature at the sites of immunization and/or elicitation of contact hypersensitivity result in differences in cell trafficking, vasodilatation or other local changes altering the response that are unrelated to changes in helper T cells. The actual mechanisms responsible for the changes in CHS response in these mice is of considerable interest and should be investigated in the near future. A more complete understanding of the role of CGRP in CHS may have important therapeutic implications. Also, future experiments with reciprocal skin grafts between control and EC RAMP1 KO mice followed by hapten application to the grafts for immunization may allow for a determination of whether CGRP signaling in ECs in the skin itself or elsewhere in the animals (secondary lymphoid organs?) is responsible for the functional changes observed in vivo. The possibility that CGRP signaling through circulating endothelial progenitor cells (EPCs) could also be considered. These cells have immunoregulatory properties including down-regulation of CD4⁺ T cell activation (29). The relevance of (EPCs) to CHS responses in vivo and the role of possible CGRP signaling through EPCs remains unknown but is an important area for future study.

Release or non-release of CGRP by peripheral nerves likely represents an important locus of modulation of immunity by the nervous system. In this regard, innervation is important

for the expression of certain inflammatory skin disorders, most notably psoriasis, and this pathway may be a mechanism by which the nervous system regulates inflammatory skin disorders. Interruption of CGRP-signaling at ECs may be a potential therapeutic target for the treatment of Th17-mediated skin diseases such as psoriasis, as well as contact hypersensitivity. It is possible that therapeutic manipulation of this pathway might also be useful for inflammatory or immune disorders in organs other than the skin.

These results convincingly demonstrate the role of CGRP regulation of immunity *in vivo*. However, they leave a number of questions unanswered. With regard to the experiments involving EC-RAMP1 KO mice, the locus of CGRP EC signaling within the mouse is unknown. It may reside in the skin, secondary lymph node organs or, perhaps, elsewhere. This must be worked out. In the experiments utilizing the inhibitor of CGRP signaling, the locus of action also remains unknown. Further investigations of regulation of immunity by CGRP-signaling will shed additional light on the role of this molecule in physiologic and pathophysiologic immune processes and may lead to novel therapeutic approaches for some inflammatory disorders.

Supplementary Material

Refer to Web version on PubMed Central for supplementary material.

Acknowledgements

We thank Willie Mark, Ph.D. and Yun You, Ph.D. for their invaluable contributions in helping to engineer and breed the inducible, conditional RAMP1 knock-out mouse employed in this project. We also thank Xuan Wang, M.D., Ph.D. for reviewing the histologic sections of EC RAMP1 KO and Cre⁻ mouse skin.

Funding for this project came from the United States National Institutes of Health grants UL1 TR002384 (X.K.Z.), and R21 AR064907 (R.D.G), a grant from the Leo Foundation and support from the Filomen M. D'Agostino Foundation and the Seth Sprague Charitable and Educational Foundation.

References

1. Breimer LH, MacIntyre I, and Zaidi M. 1988. Peptides from the calcitonin genes: molecular genetics, structure and function. *Biochem. J* 255: 377–390. [PubMed: 3060108]
2. Wimalawansa SJ. 1997. Amylin, calcitonin gene-related peptide, calcitonin, and adrenomedullin: a peptide superfamily. *Crit. Rev. Neurobiol* 11: 167–239. [PubMed: 9209829]
3. Molander C, Ygge J, and Dalsgaard CJ. 1987. Substance P-, somatostatin- and calcitonin gene-related peptide-like immunoreactivity and fluoride resistant acid phosphatase-activity in relation to retrogradely labeled cutaneous, muscular and visceral primary sensory neurons in the rat. *Neurosci. Lett* 74: 37–42. [PubMed: 2436105]
4. Ding W, Stohl LL, Xu L, Zhou XK, Manni M, Wagner JA, and Granstein RD. 2016. Calcitonin gene-related peptide-exposed ECs bias Ag presentation to CD4+ T cells toward a Th17 response. *J. Immunol* 196: 2181–2194. [PubMed: 26829986]
5. Granstein RD, Wagner JA, Stohl LL, and Ding W. 2015. Calcitonin gene-related peptide: key regulator of cutaneous immunity. *Acta. Physiol. (Oxf.)* 213: 586–594. [PubMed: 25534428]
6. Russell FA, King R, Smillie S-J, Kodji X, and Brain SD. 2014. Calcitonin gene-related peptide: physiology and pathophysiology. *Physiol. Rev* 94: 1099–1142. [PubMed: 25287861]
7. Franco-Cereceda A, Henke H, Lundberg JM, Petermann JB, Hökfelt T, and Fischer JA. 1987. Calcitonin gene-related peptide (CGRP) in capsaicin-sensitive substance P-immunoreactive sensory neurons in animals and man: distribution and release by capsaicin. *Peptides* 8:399–410. [PubMed: 2438668]

8. Kresse A, Jacobowitz DM, and Skofitsch G. 1995. Detailed mapping of CGRP mRNA expression in the rat central nervous system: comparison with previous immunocytochemical findings. *Brain Res. Bull* 36: 261–274. [PubMed: 7697380]
9. Linscheid P, Seboek D, Schaer DJ, Zulewski H, Keller U, and Müller B 2004. Expression and secretion of procalcitonin and calcitonin gene-related peptide by adherent monocytes and by macrophage-activated adipocytes. *Crit. Care Med* 32: 1715–1721. [PubMed: 15286549]
10. He Y, Ding G, Wang X, Zhu T, and Fan S. 2000. Calcitonin gene-related peptide in Langerhans cells in psoriatic plaque lesions. *Chin. Med. J. (Engl.)* 113: 747–751. [PubMed: 11776062]
11. Hou Q, Barr T, Gee L, Vickers J, Wymer J, Borsani E, Rodella L, Getsios S, Burdo T, Eisenberg E, Guha U, Lavker R, Kessler J, Chittur S, Fiorino D, Rice F, and Albrecht P. 2011. Keratinocyte expression of calcitonin gene-related peptide β : implications for neuropathic and inflammatory pain mechanisms. *Pain* 152: 2036–2051. [PubMed: 21641113]
12. Ding W, Stohl LL, Wagner JA, Granstein RD. 2008. Calcitonin gene-related peptide biases Langerhans cells toward Th2-type immunity. *J. Immunol* 181: 6020–6026. [PubMed: 18941191]
13. Mikami N, Matsushita H, Kato T, Kawasaki R, Sawazaki T, Kishimoto T, Ogitani Y, Watanabe K, Miyagi Y, Sueda K, Fukada S-O, Yamamoto H, and Tsujikawa K. 2011. Calcitonin gene-related peptide is an important regulator of cutaneous immunity: effect on dendritic cell and T cell functions. *J. Immunol* 186: 6886–6893. [PubMed: 21551361]
14. Norihisa M, Fukada S-I, Yamamoto H, and Tsujikawa K. 2012. Neuronal derivative mediators that regulate cutaneous inflammations. *Crit. Rev. Immunol* 32: 307–320. [PubMed: 23237507]
15. Gomes RN, Castro-Faria-Neto HC, Bozza PT, Soares MBP, Shoemaker CB, David JR, and Bozza MT. 2005. Calcitonin gene-related peptide inhibits local acute inflammation and protects mice against lethal endotoxemia. *Shock* 24: 590–594. [PubMed: 16317392]
16. Raud J, Lundeberg T, Brodda-Jansen G, Theodorsson E, and Hedqvist P. 1991. Potent anti-inflammatory action of calcitonin gene-related peptide. *Biochem. Biophys. Res. Commun* 180: 1429–1435. [PubMed: 1719983]
17. Clementi G, Amico-Roxas M, Caruso A, Catena Cutuli VM, Prato A, Maugeri S, de Bernardis E, and Scapagnini U. 1994. Effects of CGRP in different models of mouse ear inflammation. *Life Sci.* 54, PL119–PL124. [PubMed: 8107527]
18. Clementi G, Caruso A, Cutuli VM, Prato A, de Bernardis E, Fiore CE, and Amico-Roxas M. 1995. Anti-inflammatory activity of amylin and CGRP in different experimental models of inflammation. *Life Sci.* 57: PL193–PL197. [PubMed: 7564878]
19. Huang J, Stohl LL, Zhou X, Ding W, and Granstein RD. 2011. Calcitonin gene-related peptide inhibits chemokine production by human dermal microvascular ECs. *Brain Behav. Immun* 25: 787–799. [PubMed: 21334428]
20. Lee SH, Tonello R, Im S-T, Jeon H, Park J, Ford Z, Davidson S, Kim YH, Park C-K, and Berta T. 2020. Resolvin D3 controls mouse and human TRPV1-positive neurons and preclinical progression of psoriasis. *Theranostics* 10: 12111–12126. [PubMed: 33204332]
21. Amalia SN, Uchiyama A, Baral H, Inoue Y, Yamazaki S, Fujiwara C, Sekiguchi A, Yokoyama Y, o Ogino S, Torii R, Hosoi M, Ishikawa O, and Motegi S-I. 2021. Suppression of neuropeptide by botulinum toxin improves imiquimod-induced psoriasis-like dermatitis via the regulation of neuroimmune system. *J. Dermatol. Sci* 101: 58–68. [PubMed: 33176965]
22. Zhu TH, Nakamura M, Farahnik B, Abrouk M, Lee K, Singh R, Gevorgyan A, Koo J, and Bhutani T. 2016. The role of the nervous system in the pathophysiology of psoriasis: A review of cases of psoriasis remission or improvement following denervation injury. *Am. J. Clin. Dermatol* 17: 257–263. [PubMed: 26935938]
23. Farber EM, Lanigan SW, and Boer J. 1990. The role of cutaneous sensory nerves in the maintenance of psoriasis. *Int. J. Dermatol* 29: 418–420. [PubMed: 2397964]
24. Mulherin D, Bresnihan B, and FitzGerald O. 1995. Digital denervation associated with absence of nail and distal interphalangeal joint involvement in psoriatic arthritis. *J. Rheumatol* 22: 1211–1212.
25. Kane D, Lockhart JC, Balint P, Mann C, Ferrell WR, and McInnes IB. 2005. Protective effect of sensory denervation in inflammatory arthritis (evidence of regulatory neuroimmune pathways in the arthritic joint). *Ann. Rheum. Dis* 64: 325–327. [PubMed: 15155371]

26. Hay DL, Garelja ML, Poyner DR, and Walker CS. 2018. Update on the pharmacology of calcitonin/CGRP family of peptides: IUPHAR Review 25. *Br. J. Pharmacol* 175: 3–17. [PubMed: 29059473]
27. Liu T, Li S, Ying S, Tang S, Ding Y, Li Y, Qiao J, and Fan H. 2020. The IL-23/IL-17 pathway in inflammatory skin diseases: From bench to bedside. *Front. Immunol* 11: 594735. [PubMed: 33281823]
28. Reich A, Orda A, Wi nicka B, and Szepietowski JC. 2007. Plasma concentration of selected neuropeptides in patients suffering from psoriasis. *Exp. Dermatol* 16: 421–428. [PubMed: 17437485]
29. Naserian S, Abdelgawad ME, Bakshloo MA, Ha G, Arouche N, Cohen JL, Salomon BL, and Uzan G. 2020. The TNF/TNFR2 signaling pathway is a key regulatory factor in endothelial progenitor cell immunosuppressive effect. *Cell Commun. Signal* 18: 94. [PubMed: 32546175]

Key Points

CGRP signaling at ECs regulates Th cell responses in regional lymph nodes in vivo.

CGRP signaling at ECs plays a key role in the CHS response.

The EC CGRP signaling locus might prove useful for therapeutic manipulation.

Author Manuscript

Author Manuscript

Author Manuscript

Author Manuscript

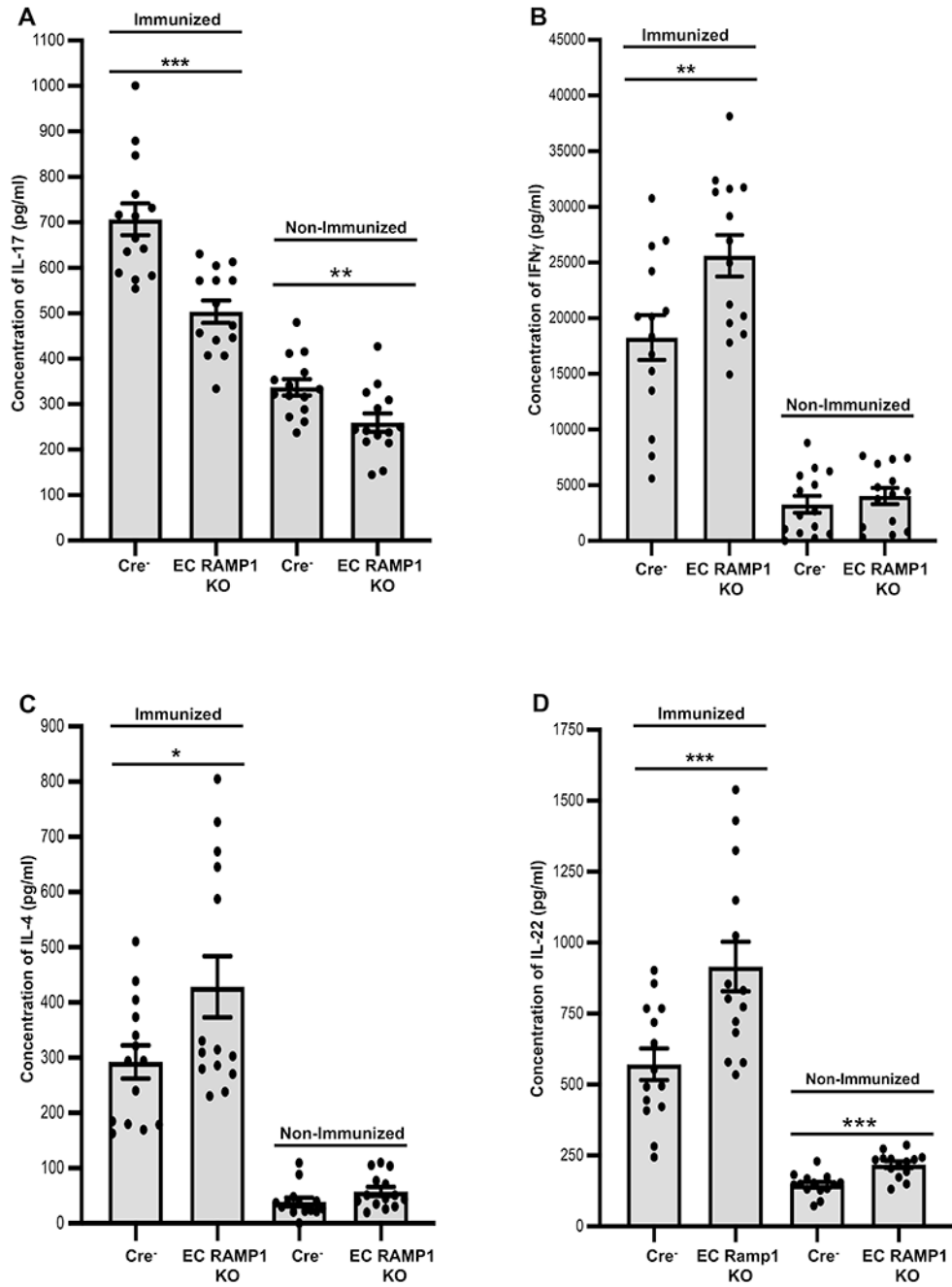


FIGURE 1.

CGRP signaling through ECs regulates regional lymph node CD4⁺ T cell cytokine production after immunization of mice. Mice were immunized to DNFB or mock-immunized on the shaved dorsa of groups of EC RAMP1 KO and Cre⁻ mice. Three days later, mice were euthanized and draining of lymph nodes harvested. A single-cell suspension of CD4⁺ T cells from the draining lymph nodes was prepared and cells were placed in culture and stimulated with anti-CD3 and anti-CD28 mAbs. Supernatants were harvested after 72-hours and assayed by ELISA for cytokine content. Cells from immunized EC

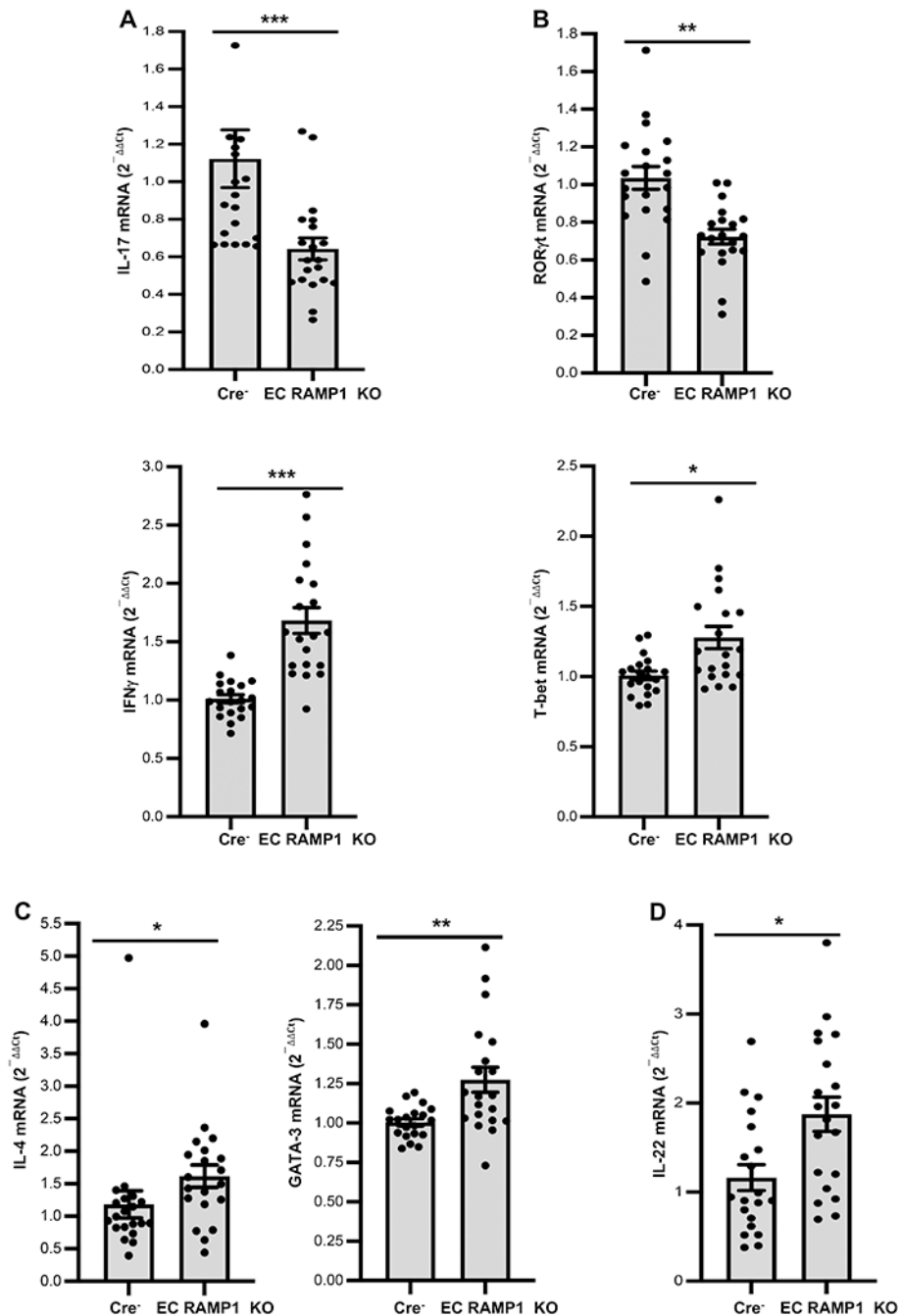
Author Manuscript

Author Manuscript

Author Manuscript

Author Manuscript

RAMP1 KO mice produced significantly less **(A)** IL-17A compared to immunized Cre⁻ control mice and a small but a significant reduction was also seen in non-immunized mice while production of **(B)** IFN- γ , **(C)**, IL-4, and **(D)** IL-22 was significantly increased. **(D)** IL-22 also showed a significant increase in non-immunized mice. Bars represent mean \pm SEM. * $p < 0.05$, ** $p < 0.01$, *** $p < 0.001$. N=10/group, dots represent individual mouse values. Measurements were taken from CD4⁺ cells from distinct mice, aggregated from 2 separate experiments.

**FIGURE 2.**

CGRP signaling through ECs regulates regional lymph node CD4⁺ T cell mRNA levels of cytokines and transcription factors after immunization of mice. Groups of EC RAMP1 KO and Cre⁻ mice were immunized to DNFB or mock-immunized on the shaved dorsa as in Materials and Methods. Three days later, mice were euthanized and draining of lymph nodes harvested. Total RNA was isolated from draining lymph node CD4⁺ T cells and real-time PCR for IL-17A and RORγt mRNAs, IFN-γ and T-bet expression performed. mRNA levels for (A) IL-17A and RORγt were significantly reduced in EC RAMP1 KO mice

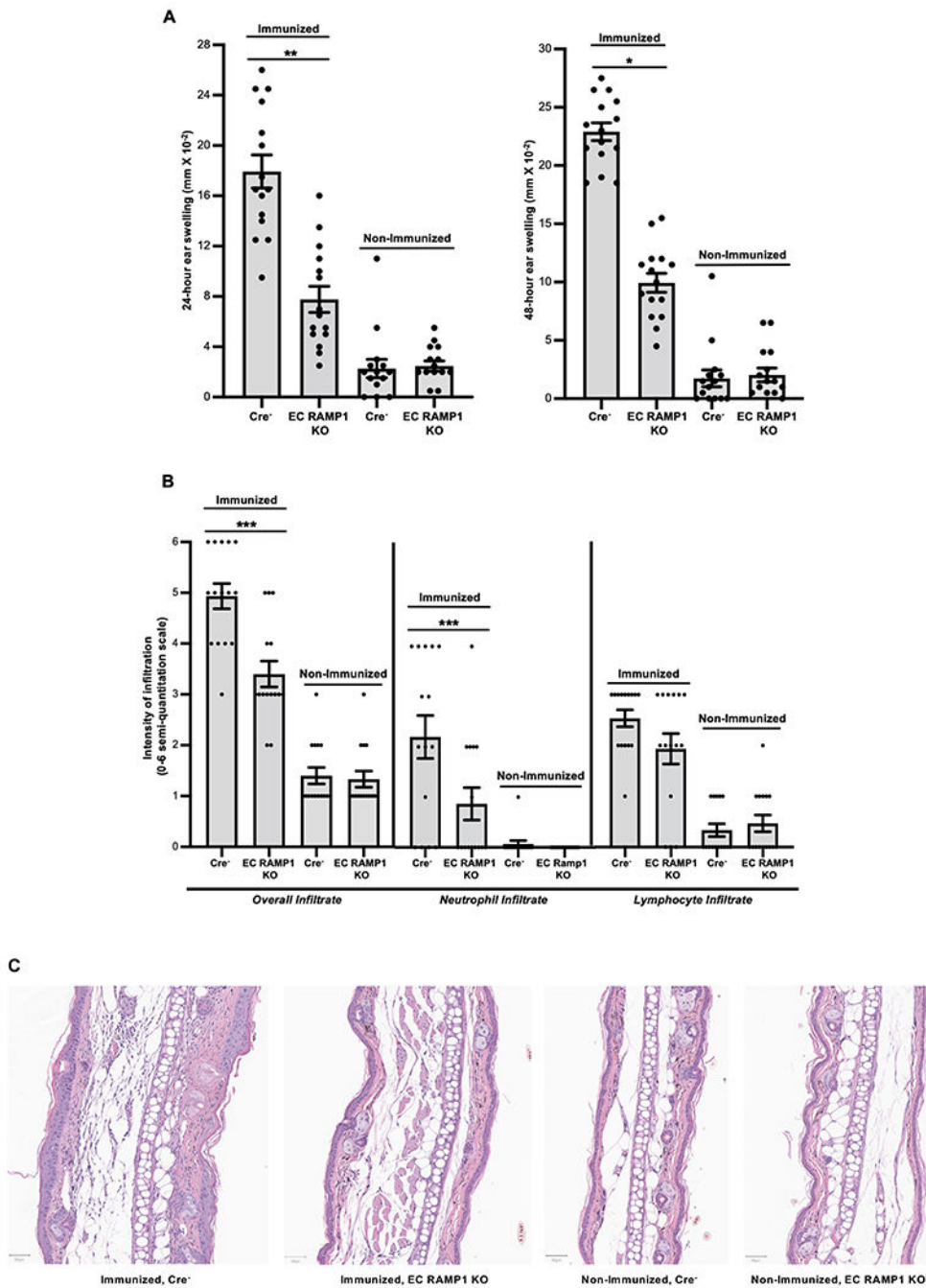
while mRNA levels for **(B)** IFN- γ , **(B)** T-bet, **(C)** IL-4, **(C)** GATA3 and **(D)** IL-22 were significantly increased. Bars represent mean \pm SEM. * $p < 0.05$, ** $p < 0.01$, *** $p < 0.001$. N=10/group, dots represent individual mouse values. Measurements were taken from CD4⁺ cells from distinct mice, aggregated from 2 separate experiments.

Author Manuscript

Author Manuscript

Author Manuscript

Author Manuscript

**FIGURE 3.**

Interruption of CGRP signaling through ECs significantly inhibits contact hypersensitivity in mice. EC RAMP1 KO and Cre⁻ mice were each immunized by application of DNFB to the shaved dorsum or were mock-immunized with diluent alone. Seven days later, mice were challenged by application of DNFB to the ears and the CHS response quantified by measurement of 24- and 48-hour ear swelling. (A) Immunized EC RAMP1 KO mice had a substantial and significantly lesser CHS response compared to Cre⁻ control mice. Bars represent mean \pm SEM. * $p < 0.05$, ** $p < 0.01$. N=15/group, dots represent individual

mouse values. Measurements were taken from distinct mice, aggregated from 3 separate experiments. **(B)** Histologic assessment of the ears harvested at 48 hours revealed a significant reduction in the total inflammatory cell response, a significant reduction in the neutrophil infiltrate and a trend toward a lessor lymphocyte infiltrate in ear skin from immunized EC RAMP1 KO mice compared to Cre⁻ mice. Bars represent mean +/- SEM. ***p<0.001. N=15/group, dots represent individual mouse values. Measurements were taken from distinct mice, aggregated from 3 separate experiments. **(C)** Photomicrographs of a representative section from the ear of a mouse from each group taken 48-hours after challenge (Immunized Cre⁻, Immunized EC RAMP1 KO, Non-Immunized Cre⁻ and Non-Immunized EC RAMP1 KO). Note that the ear from the immunized Cre⁻ mouse is thicker than the ear from the immunized EC RAMP1 KO with more edema and a thicker dermis with greater inflammatory cell infiltrate. Bar represents 50 µm in each photomicrograph.

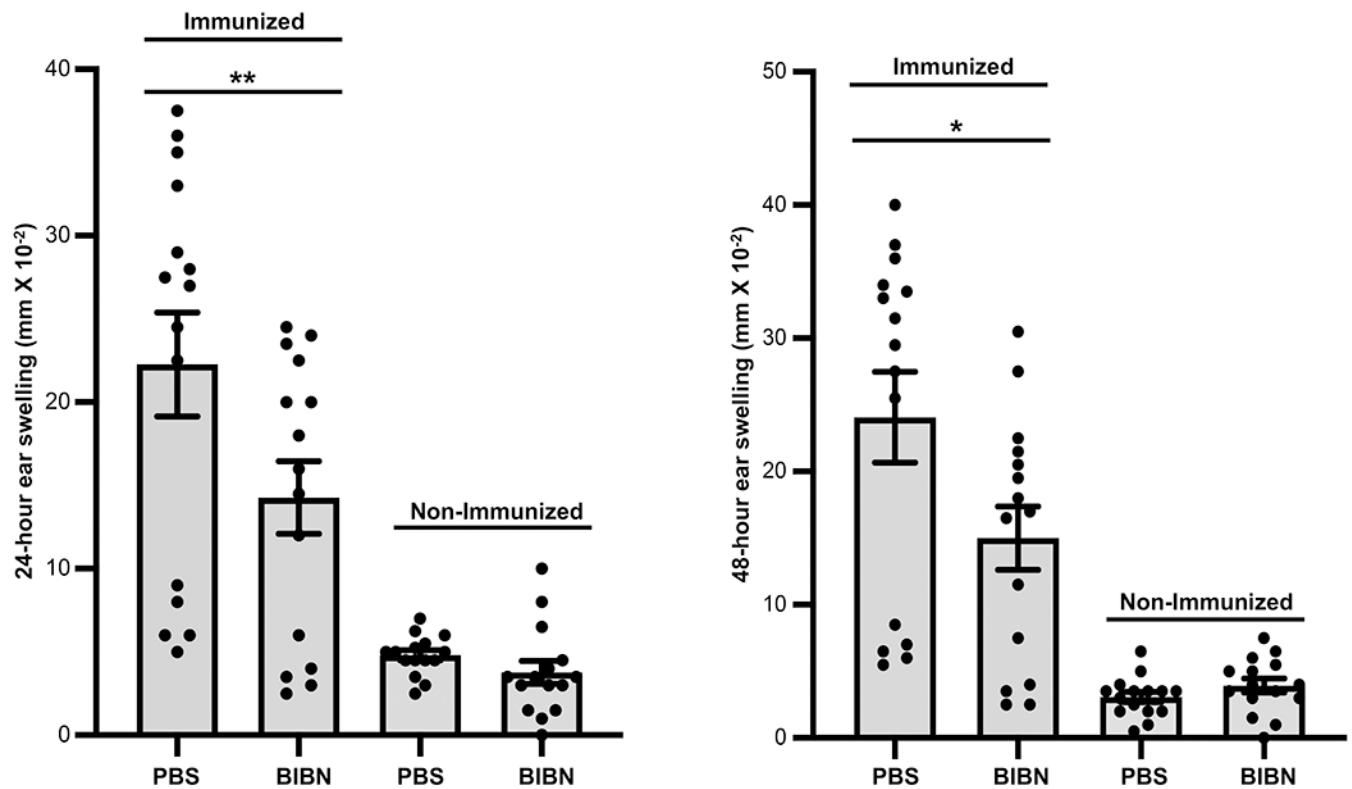


FIGURE 4.

Systemic administration of a competitive inhibitor of CGRP significantly inhibits contact hypersensitivity in mice. Wild-type mice were injected intraperitoneally with the CGRP inhibitor (BIBN) one hour before and one hour after immunization with DNFB by application to the shaved dorsum or were mock-immunized with diluent alone. One-week later BIBN was injected into the base of each ear followed 30 minutes later by challenge of each ear with application of DNFB and 24- and 48-hr ear swelling assessed. Control mice were similarly treated but injected with diluent alone instead of BIBN. Other groups of control mice were treated identically to the groups described above but were mock-immunized with vehicle alone. Immunized mice injected with BIBN exhibited a significantly reduced CHS response compared to immunized control mice injected with PBS alone. Bars represent mean \pm SEM. * $p < 0.05$, ** $p < 0.01$. $N = 15$ /group, dots represent individual mouse values. Measurements were taken from CD4⁺ cells from distinct mice, aggregated from 3 separate experiments.